# Comparison of Corneal Morphologic Parameters and High Order Aberrations in Keratoconus and Normal eyes

J.S. Velázquez[1[0000-0002-1329-5093]], F. Cavas[1*[0000-0002-8391-0688]], J.M. Bolarín[2[0000-0003-2400-9213]] and J. Alió[3,4[0000-0002-8082-1751]]

[1] Department of Structures, Construction and Graphic Expression, Technical University of Cartagena, 30202 Cartagena, Spain
[2] Technology Centre for IT and Communications (CENTIC), Scientific Park of Murcia, 30100 Murcia, Spain
[3] Keratoconus Unit of Vissum Corporation Alicante, 03016 Alicante, Spain
[4] Department of Ophthalmology, Miguel Hernández University of Elche, 03202 Alicante, Spain
francisco.cavas@upct.es

**Abstract.** The aim of this study is evaluating the influence of corneal geometry in the optical system's aberrations, and its usefulness as diagnostic criterion for keratoconus.159 normal eyes (normal group, mean age 37.8 ± 11.6 years) and 292 eyes with the diagnosis of keratoconus (keratoconus group, mean age 42.2 ± 17.6 years) were included in this study. All eyes received a comprehensive ophthalmologic examination. A virtual 3D model of each eye was made using CAD software and different anatomical parameters related with surface and volume were measured. Statistically significant differences were found for all anatomical parameters (all $p < 0.001$). AUROC analysis showed that all parameters reached values above 0.7, with the exception of the total corneal surface area (TCSAA-S). In conclusion, the methodology explained in this research, that bases in anatomical parameters obtained from a virtual corneal model, allow to analyze the diagnostic value of corneal geometry correlation with optical aberrations in keratoconus pathology.

**Keywords:** Ophthalmology, Corneal Apex, Computer-Aided Design (CAD), Computational Modelling, Scheimpflug Technology.

## 1 Introduction

The human eye is an optical instrument that projects images from outside into the retina [1]. However, the eye is characterized by a lack of symmetry in its surfaces, as these do not present revolution symmetry because of their de-alignment and de-centration. This causes a degradation in the quality of image by means of aberrations of the optical system [2,3]. This refractive anomaly can elicit the well-known astigmatism, myopia or hyperopia in patients.

In keratoconus (KCN) disease, that is an affection in which the cornea acquires a conical structure as a result of a progressive corneal thinning [4], corneal thickness reduction causes optical aberrations.

There are different indices for the detection of KCN basing on astigmatism [5], like the AST or the SRAX index. Both quantify irregular astigmatism, but these indices are characterized for using only data of the anterior surface of the cornea. Other authors [6,7] use wave-front based technologies to detect astigmatism, yet it has been demonstrated that aberrations are difficult to measure with these methods, as they do not cover the whole corneal surface. Consequently, it would be interesting to measure astigmatism from geometrical data obtained from the corneal topographies, as this data in fact register almost completely anterior and posterior corneal surfaces.

Our research group has validated a geometrical patient-specific virtual model for the diagnosis of KCN from a morpho-geometric point of view [8,9,2,10]. This patient-specific model has been used in other fields, such as the Finite Elements one [11-14], in which it has been used to analyze the biomechanical behavior of the cornea to refractive surgeries or the response to the intra-stromal ring segment implantation in corneas with keratoconus [11,13], and also to analyze the behavior of corneal tissue properties in different scenarios [14].

Also, there are many different approaches in which KCN classification can be based, usually relying in lens refraction, corneal thickness, keratometry data, corrected distance visual acuity (CDVA), internal astigmatism, root mean square, central keratometry, corneal asphericity at 8 mm, pachymetry and myopia, among others [5]. This study proposes using a classification based in high order aberrations (HOA), the one known as Alió-Shabayek [15].

Therefore, in this research work it is evaluated the influence of the corneal geometry in optical aberrations, and its usefulness as a criterion for the diagnosis of keratoconus.

## 2 Patients and Methods

### 2.1 Patients

A total number of 451 eyes of 451 individuals with ages ranging from 16 to 75 years were evaluated at Vissum Hospital (Alicante). All the procedures adhered to the tenets of the Declaration of Helsinki (Fortaleza, 2013) and were approved by the Ethical Board of the hospital. All patients were informed and authorized their inclusion in the study by signing an informed consent. These data are included in the “Iberia” database of KCN eyes created for the National Network for Clinical Research in Ophthalmology RETICS-OFTARED.

A thorough and detailed ophthalmic exam was made to all the subjects [10] and they were divided into two different groups (normal and keratoconus) according to the Alió-Shabayek grading system [15].

The first group did not present any ocular pathology and consisted in 159 healthy eyes of 159 patients (89 men / 70 women, mean age 37.8 ± 11.6). Inclusion criterion was: any patient who did not present any ocular or corneal pathology. Exclusion criterion was: patient whose eyes had undergone any previous surgical procedure.

The second group corresponded to diseased eyes, and consisted in 292 eyes of 292 patients. (162 men / 130 women, mean age 42.2 ± 17.6). Inclusion criterion was:

presence of a localized corneal topography steepening and / or the presence of an asymmetric bow tie with or without topographical angulated principal meridians, and any microscopic keratoconic sign: Fleischer ring, Vogt striae, stromal thinning, protrusion apex or anterior corneal scars in the corneal stroma. Exclusion criterion was: any previous eye surgical procedure and any other eye pathology different from the keratoconus.

### 2.2 Methods

The procedure followed in our research work can be described by two main phases (see Fig. 1): a first phase of 3D corneal model generation and a second one of geometrical analysis of the 3D model.

**First Phase.** Systems based on the projection of a slit of light onto the cornea and on the principle of Scheimpflug photography [5] allow the exportation of data containing the geometrical readings of each specific patient. These data are known as "raw data" [8,9], and are used to create patient-specific models [8,9,2,13,14,10] in the fields of Finite Elements and Computer-Aided Design.

In our study, we have used Sirius tomographer (Construzione Strumenti Oftalmici, Italy), a device based in principle of Scheimpflug photography, that allows the characterization of the optical aberrations present in the patient's eye, as well as the exportation of geometrical data into a .CSV format file. [14]. These data are transformed into Cartesian coordinates, as we are working with a set of spatial points (see Fig. 1), so our team has programmed an algorithm using Matlab® V R2014 software (Mathworks, Natick, USA), in order to:

- Transform the set of spatial data given in polar coordinates in the .CSV file to a set of spatial data in Cartesian format in a .TXT file (see Figure 1, First Phase). We made this transformation because Rhinoceros® V 5.0 software (MCNeel & Associates, Seattle, USA) uses this set of spatial data in Cartesian format to generate the corneal surfaces.
- b) Validate those sets of spatial data that present invalid reading values of the corneal surface's geometry (see Figure 2). Due to the existence of factors extrinsic to the patient while measures are being taken [5], like tear film stability, tabs that block the visual field or improper opening of the eyelids, data acquired by the Sirius device for determined points located in the peripheral zones can be not valid, getting in those cases a value of −1000 in the corresponding matrix cells. To avoid including these invalid cyphers, all the CSV files created for each cornea went through a filtering process, being selected for this research just those cases that held correct values in their first 21 rows (256 values per row; radii values ranging from 0 mm to 4 mm in reference to the normal corneal vertex), discarding from the research any cornea that included invalid −1000 values located within this range. This filtering procedure guaranteed that all data utilized for generating clouds of points was real, and interpolation was not used [8,9,16].

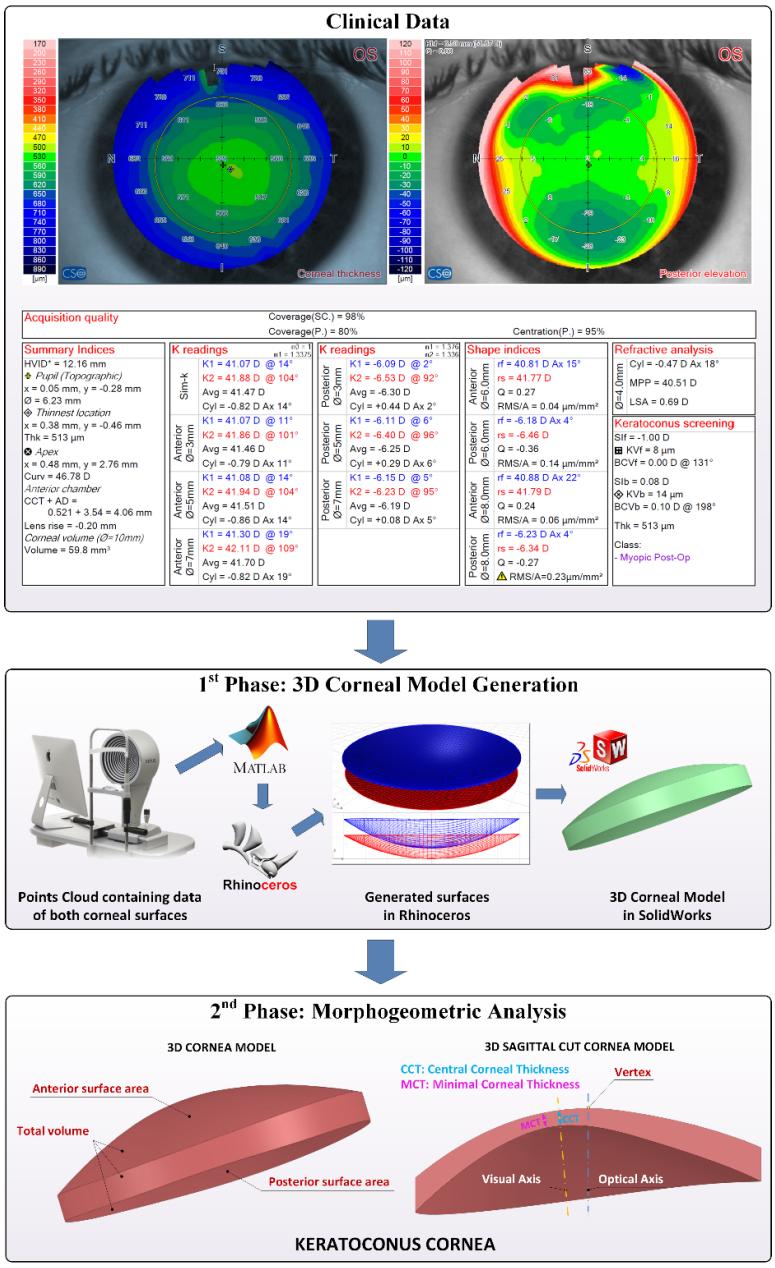


**Fig. 1.** Procedure followed for the 3D corneal model generation and later analysis. Data obtained from Sirius tomographer allow the generation of a personalized 3D model, in which several morphogeometric variables are studied.

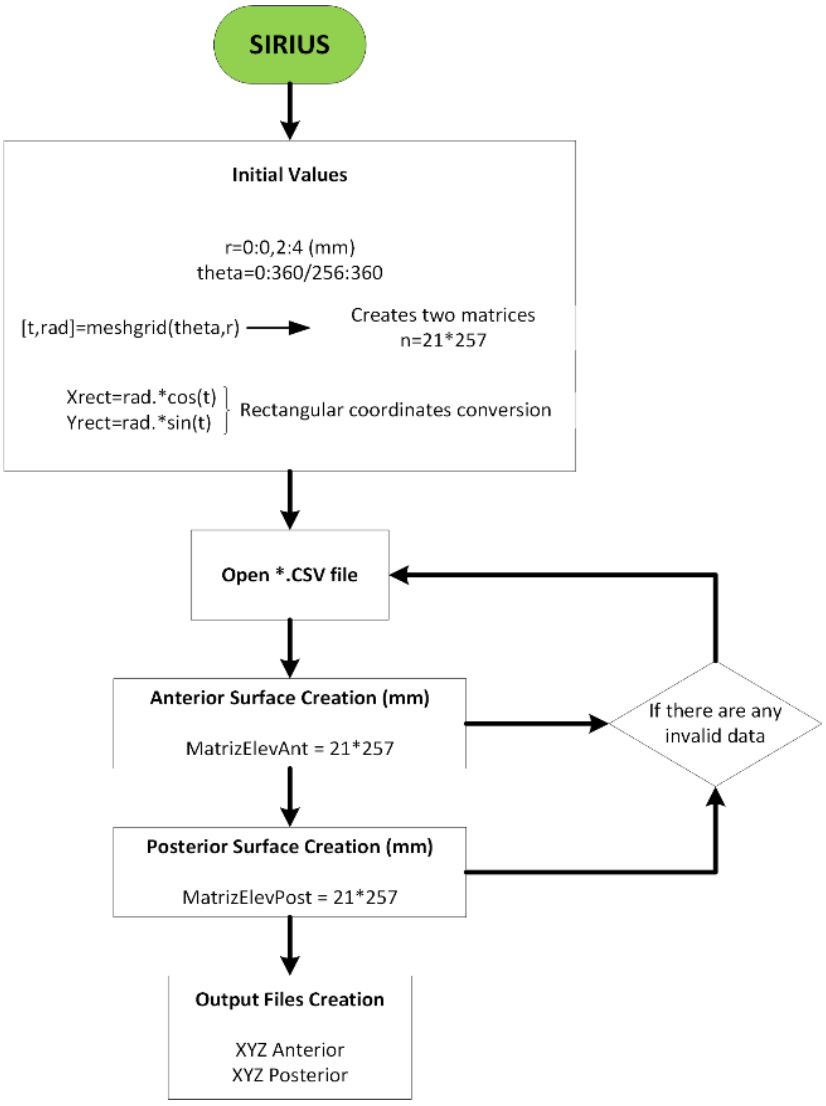


**Fig. 2.** Description of the algorithm followed for the coordinate transformation

Once anterior and posterior surfaces of the cornea have been generated in Rhinoceros®, they are both exported into SolidWorks V2017 software (Dassault Systèmes, Vélizy-Villacoublay, France) to create a complete 3D model of the cornea.

**Second Phase.** Over the 3D model and within the graphical environment of the modelling software, a structural characterization of the corneal morphology was done through a geometrical analysis of the model, that was made with the measurement tools integrated in the program. These tools allow the definition of a set of variables

of superficial and volumetric nature that have already been used in previous works (see Table 1), although it is the first time that they are used to evaluate the influence of corneal geometry in optical aberrations.

**Table 1.** Set of geometrical parameters analyzed for the Alió-Shabayek classification. [10]

| *Geometric variable* | *Description* |
|---|---|
| Total corneal volume ($TCV_{A\text{-}S}$) [$mm^3$] | Volume limited by front, back and peripheral surfaces of the solid model generated |
| Anterior corneal surface area ($ACSA_{A\text{-}S}$) [$mm^2$] | Area of the front/exterior surface |
| Posterior corneal surface area ($PCSA_{A\text{-}S}$) [$mm^2$] | Area of the rear/interior surface |
| Total corneal surface area ($TCSA_{A\text{-}S}$) [$mm^2$] | Sum of anterior, posterior and perimetral corneal surface areas of the solid model generated |
| Sagittal plane apex area ($SPAP_{A\text{-}S}$) [$mm^2$] | Area of the cornea within the sagittal plane passing through the optical axis and the highest point (apex) of the anterior corneal surface |
| Sagittal Plane Area in minimum thickness point ($SPAMTP_{A\text{-}S}$) [$mm^2$] | Area of the cornea within the sagittal plane passing through the optical axis and the minimum thickness point (maximum curvature) of the anterior corneal surface |
| Corneal volume R-x ($CV_{A\text{-}S}$ R-x) [$mm^3$] | Corneal volume R-x defined by the anterior corneal apex at radii 0.5, 1.0 and 1.5 mm |

### 2.3 Statistical Analysis

Just a single eye per patient was selected in a dichotomous sequence (0 and 1), made by a computer software, to elude any potential correlations between eyes of the same patient Graphpad Prism v7.0 for MAC OS X (Graphpad Inc., La Jolla, USA) and SPSS 24.0 software (SPSS Inc., Chicago, USA) were the two software chosen for the analysis of the data. Data normality was tested by means of Kolmogovov-Smirnov test. Comparison between groups was performed by one-way analysis of variance (ANOVA) if variables were normally distributed, whereas Kruskal-Wallis non-parametric test was used for non-normally distributed ones. Bonferroni test was selected for post-hoc comparative analysis for the ANOVA when the variances were homogeneous and T2 Tamhane test was the option when variances did not show homogeneity. P-values $< 0.05$ were considered statistically significant for the differences. Lastly, receiver operating characteristic (ROC) curves were used to determine which parameters better characterized diseased corneas.

## 3 Results

This study comprised a total number of 451 eyes: 159 healthy eyes (35.25%) and 292 (64.75%) diagnosed as suffering from KCN according to the Alió-Shabayek grading scale, presenting High Order Aberrations (HOA) of third order.

With respect to the healthy eyes, 74 individuals were men (46.5%) and 85 were women (53.5%), being 82 right eyes (51.4%) and 76 left eyes (49.6%).

Clinical data that these individuals presented for optical aberrations were: Root Mean Square High Order Aberrations (RMS HOA) was 0.41 µm (range 0.23 to 0.73 µm); Spherical Aberration (SA) was 0.23 µm (range 0.07 to 0.43 µm); Root Mean Square Coma (RMS Coma) was 0.30 µm (range 0.03 to 0.69 µm); Root Mean Square Coma-like was 0.35 µm (range 0.09 to 0.72 µm) and Root Mean Square Spherical-like was 0.25 µm (range 0.10 to 0.50 µm).

Finally, regarding astigmatism, corneal asphericity was calculated at 4.5 mm and at 8 mm. In this respect, the one at 4.5 mm was -0.1 (range -0.62 to 0.87) and the one at 8 mm was -0.28 (range -0.70 to 0.17).

With respect to the eyes diagnosed as KCN, 125 subjects were men (42.8%) and 167 were women (57.2%), being 134 right eyes (45.8%) and 158 left eyes (55.2%).

Clinical data that these individuals presented for optical aberrations were: Root Mean Square High Order Aberrations (RMS HOA) was 2.6 µm (range 0.33 to 13.9 µm); Spherical Aberration (SA) was -0.19 µm (range -7.9 to 1.40 µm); Root Mean Square Coma (RMS Coma) was 2.1 µm (range 0.05 to 12.9 µm); Root Mean Square Coma-like was 2.34 µm (range 0.21 to 13.01 µm) and Root Mean Square Spherical-like was 0.89 µm (range 0.14 to 8.3 µm).

As with the healthy group, corneal asphericity was calculated at 4.5 mm and at 8 mm, being at 4.5 mm -0.6 (range -7.39 to 4.09) and at 8 mm -0.81 (range -3.0 to 2.85).

Analyzing descriptive values and their differences when comparing healthy and KCN eyes (see Table 2), all the geometrical variables ($p < 0.05$) showed good capability of discrimination between groups, without exceptions.

**Table 2.** Descriptive values and differences in the modelled geometric variables among the normal and keratoconus groups. SD: standard deviation. P: statistical test.

| *Measurement* | *Normal Group (n = 159)* | | | | *Keratoconus Group (n = 292)* | | | | | |
|---|---|---|---|---|---|---|---|---|---|---|
| | *Mean* | *SD* | *Min* | *Max* | *Mean* | *SD* | *Min* | *Max* | *z* | *P* |
| $TCV_{A\text{-}S}$ ($mm^3$) | 25.55 | 1.58 | 25.51 | 25.61 | 23.91 | 1.89 | 23.85 | 23.96 | 25.08 | <0.001 |
| $ACSA_{A\text{-}S}$ ($mm^2$) | 43.10 | 0.15 | 43.07 | 43.14 | 43.45 | 0.54 | 43.32 | 43.64 | 175.59 | <0.001 |
| $PCSA_{A\text{-}S}$ ($mm^2$) | 44.27 | 0.30 | 44.22 | 44.32 | 44.82 | 0.87 | 44.69 | 44.99 | 151.62 | <0.001 |
| $TCSA_{A\text{-}S}$ ($mm^2$) | 103.87 | 1.18 | 103.81 | 103.91 | 104.07 | 1.99 | 104.01 | 104.16 | 36.16 | <0.001 |
| $SPAP_{A\text{-}S}$ ($mm^2$) | 4.28 | 0.26 | 4.22 | 4.34 | 3.96 | 0.33 | 3.91 | 4.00 | 34.46 | <0.001 |
| $SPAMTP_{A\text{-}S}$ ($mm^2$) | 4.27 | 0.27 | 4.22 | 4.33 | 3.94 | 0.33 | 3.89 | 3.97 | 36.38 | <0.001 |
| $CV_{A\text{-}S}$ R-0.5 ($mm^3$) | 0.41 | 0.03 | 0.35 | 0.45 | 0.36 | 0.05 | 0.23 | 0.40 | 221.38 | <0.001 |
| $CV_{A\text{-}S}$ R-1 ($mm^3$) | 1.69 | 0.11 | 1.63 | 2.01 | 1.47 | 0.08 | 1.38 | 1.50 | 221.20 | <0.001 |
| $CV_{A\text{-}S}$ R-1.5 ($mm^3$) | 3.86 | 0.25 | 3.80 | 3.91 | 3.43 | 0.37 | 3.36 | 3.46 | 73.39 | <0.001 |

In addition, an area under the receiver-operator curve (AUROC) analysis was made for the nine geometrical studied variables (Fig. 3), with good values of area under the curve (above 0.7), for all variables except total corneal surface, as shown in Table 3.

**Table 3.** The area under the ROC results.

| *Measurement* | *Area* | *Sensitivity* | *Specificity* | *Standard error* | *95% Confidence Interval* | |
|---|---|---|---|---|---|---|
| | | | | | *Lower limit* | *Upper limit* |
| $TCV_{A\text{-}S}$ | 0.751 | 60.6 | 78.0 | 0.023 | 0.706 | 0.796 |
| $ACSA_{A\text{-}S}$ | 0.782 | 62.3 | 83.6 | 0.021 | 0.741 | 0.824 |
| $PCSA_{A\text{-}S}$ | 0.754 | 47.6 | 90.6 | 0.023 | 0.710 | 0.799 |
| $TCSA_{A\text{-}S}$ | 0.501 | 17.5 | 93.7 | 0.021 | 0.447 | 0.545 |
| $SPAP_{A\text{-}S}$ | 0.781 | 50.3 | 94.3 | 0.021 | 0.739 | 0.823 |
| $SPAMTP_{A\text{-}S}$ ($mm^2$) | 0.781 | 48.3 | 95.0 | 0.021 | 0.739 | 0.823 |
| $CV_{A\text{-}S}$ R-0.5 ($mm^3$) | 0.860 | 70.2 | 89.9 | 0.017 | 0.826 | 0.894 |
| $CV_{A\text{-}S}$ R-1 ($mm^3$) | 0.853 | 72.3 | 85.5 | 0.017 | 0.819 | 0.887 |
| $CV_{A\text{-}S}$ R-1.5 ($mm^3$) | 0.836 | 61.6 | 91.8 | 0.018 | 0.800 | 0.873 |

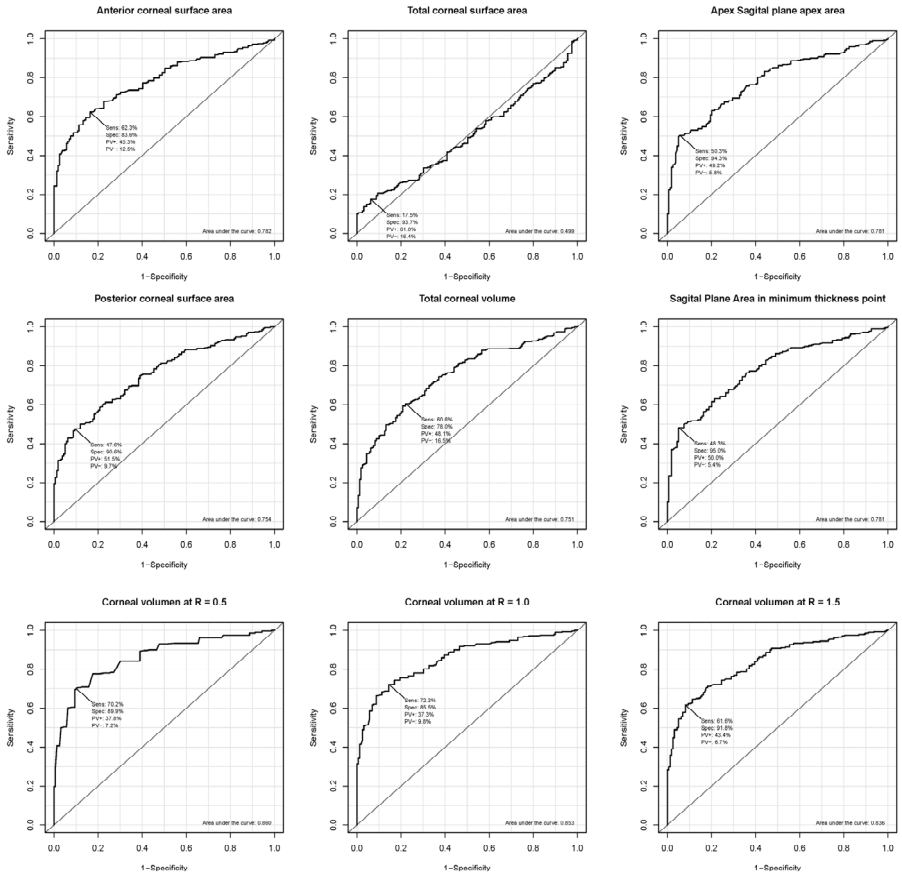


**Fig. 3.** Curves for modelled parameters detecting KC.

## 4 Discussion

Patients suffering from KCN present values in optical aberrations significantly higher than the ones of those with normal eyes [17]. This is caused by the deformation that the wave front suffers when it reaches the corneal surface, due to the de-centration of the point of maximum curvature in KCN. However, one of the aspects to which less attention has been paid is the potential diagnostic value of the optical aberrations correlated with corneal geometry in KCN pathology. This work develops a methodology that analyses the relationship between different anatomical parameters and optical aberrations.

For this study, a Sirius corneal tomographer (Construzione Strumenti Oftalmici, Italy) has been used. It is a device that provides consistent and repeatable measures for each patient [18]. In reference with the anatomical parameters studied in the virtual model, volume parameters and surface parameters should be considered separately.

Regarding the first ones, total corneal volume ($TCV_{A\text{-}S}$) presented significant differences between the studied groups, but they were not remarkable, not coinciding this result with the ones reported in other previous studies. [16,19,20]. This can be explained by the fact that the KCN group includes an important amount of eyes with advanced KCN. In addition, this result is in line with the existence of significant differences in measured corneal volumes at R = 0.5, R=1 and at R = 1.5, as the tendency of corneal structure is being more irregular or oblate (more curved) in central zone than in peripheral zone, in which it is more regular or prolate.

Regarding anatomical surface parameters, all variables presented statistically significant differences between groups, being these remarkable for anterior corneal surface area and posterior corneal surface area. This finding is in line with other studies that have used the same Sirius technology [21,20]. Piñero et al [20] proved that corneal curvature increases with disease progression, this is, the areas of both corneal surfaces grow as they become steeper. Also, Ishi et al [21] demonstrated that a correlation between surfaces existed for the more advanced degrees of the disease. An explanation of the finding in our study can be that posterior surface curves, in proportion, more than the anterior one, because of the relation of mechanical feebleness that corneal tissues present [12]. Other less significant superficial parameters were also studied, such as the sagittal areas obtained from the apex and from anterior the minimum thickness point of the cornea, although these variables were not significant for the study. This can be caused by the fact that the local change inducted by the intraocular pressure in corneal surface is not representative in these areas for the study of a wave front (aberrometry). This has been reported by our research team in previous studies [8-10].

Sensibility analysis of the measured variables revealed that some variables presented values of AUROC > 0.7, more precisely $TCV_{A\text{-}S}$ AUC, $ACSA_{A\text{-}S}$, $PCSA_{A\text{-}S}$, $SPAP_{A\text{-}S}$, $SPAMTP_{A\text{-}S}$, $CV_{A\text{-}S}$ R-0.5, $CV_{A\text{-}S}$ R-1 and $CV_{A\text{-}S}$ R-1.5. Consequently, these variables can be used for diagnosing KCN.

## 5 Conclusion

Anatomical variables of surface and volume obtained from a virtual model of the cornea for each patient allow to characterize and discriminate, in a reliable way, healthy corneas from corneas with optical aberrations, diagnosed with KCN according to the Alió-Shabayek optical classification. These anatomical variables can be a helpful tool that may allow measuring the optical quality of vision of the patients. However, the discrimination power of several variables used conjointly has not been studied in this research work, and opens a new way to explore for future ones, using techniques such as logistic regression.

## Funding

This publication has been carried out in the framework of the Thematic Network for Co-Operative Research in Health (RETICS), reference number RD16/0008/0012,

financed by the Carlos III Health Institute–General Subdirection of Networks and Cooperative Investigation Centers (R&D&I National Plan 2013–2016) and the European Regional Development Fund (FEDER).

## References

1. Hansen ED, Hartnett ME (2019) A review of treatment for retinopathy of prematurity. Expert Review of Ophthalmology 14 (2):73-87. doi:10.1080/17469899.2019.1596026
2. Cavas-Martínez F, Piñero DP, Fernández-Pacheco DG, Mira J, Cañavate FJF, Alió JL (2018) Assessment of pattern and shape symmetry of bilateral normal corneas by scheimpflug technology. Symmetry 10 (10). doi:10.3390/sym10100453
3. Giovanzana S, Kasprzak HT, Pałucki B, Ţălu Ş (2013) Non-rotational aspherical models of the human optical system. Journal of Modern Optics 60 (21):1899-1905. doi:10.1080/09500340.2013.865802
4. Salomão M, Hoffling-Lima AL, Lopes B, Belin MW, Sena N, Dawson DG, Ambrósio R (2018) Recent developments in keratoconus diagnosis. Expert Review of Ophthalmology 13 (6):329-341. doi:10.1080/17469899.2018.1555036
5. Cavas-Martinez F, De la Cruz Sanchez E, Nieto Martinez J, Fernandez Canavate FJ, Fernandez-Pacheco DG (2016) Corneal topography in keratoconus: state of the art. Eye and vision (London, England) 3:5. doi:10.1186/s40662-016-0036-8
6. Maeda N, Fujikado T, Kuroda T, Mihashi T, Hirohara Y, Nishida K, Watanabe H, Tano Y (2002) Wavefront aberrations measured with Hartmann-Shack sensor in patients with keratoconus. Ophthalmology 109 (11):1996-2003. doi:10.1016/s0161-6420(02)01279-4
7. Mihaltz K, Kranitz K, Kovacs I, Takacs A, Nemeth J, Nagy ZZ (2010) Shifting of the line of sight in keratoconus measured by a hartmann-shack sensor. Ophthalmology 117 (1):41-48. doi:10.1016/j.ophtha.2009.06.039
8. Cavas-Martínez F, Bataille L, Fernández-Pacheco DG, Cañavate FJF, Alio JL (2017) Keratoconus Detection Based on a New Corneal Volumetric Analysis. Scientific Reports 7 (1). doi:10.1038/s41598-017-16145-3
9. Cavas-Martínez F, Bataille L, Fernández-Pacheco DG, Cañavate FJF, Alió JL (2017) A new approach to keratoconus detection based on corneal morphogeometric analysis. PLoS ONE 12 (9). doi:10.1371/journal.pone.0184569
10. Velázquez JS, Cavas F, Alió Del Barrio J, Fernández-Pacheco DG, Alió J (2019) Assessment of the association between in Vivo corneal morphogeometrical changes and keratoconus eyes with severe visual limitation. Journal of Ophthalmology 2019. doi:10.1155/2019/8731626
11. Carvalho LA, Prado M, Cunha RH, Neto AC, Paranhos Jr A, Schor P, Chamon W (2009) Keratoconus prediction using a finite element model of the cornea with local biomechanical properties. Arquivos Brasileiros de Oftalmologia 72 (2):139-145. doi:10.1590/S0004-27492009000200002

12. Gefen A, Shalom R, Elad D, Mandel Y (2009) Biomechanical analysis of the keratoconic cornea. Journal of the Mechanical Behavior of Biomedical Materials 2 (3):224-236. doi:10.1016/j.jmbbm.2008.07.002
13. Lanchares E, Buey MAD, Cristóbal JA, Calvo B, Ascaso FJ, Malvè M (2016) Computational simulation of scleral buckling surgery for rhegmatogenous retinal detachment: On the effect of the band size on the myopization. Journal of Ophthalmology 2016. doi:10.1155/2016/3578617
14. Pandolfi A, Manganiello F (2006) A model for the human cornea: Constitutive formulation and numerical analysis. Biomechanics and Modeling in Mechanobiology 5 (4):237-246. doi:10.1007/s10237-005-0014-x
15. Alio JL, Shabayek MH (2006) Corneal higher order aberrations: a method to grade keratoconus. Journal of refractive surgery (Thorofare, NJ : 1995) 22 (6):539-545
16. Cavas-Martínez F, Fernández-Pacheco DG, De La Cruz-Sánchez E, Nieto Martínez J, Fernández Cañavate FJ, Vega-Estrada A, Plaza-Puche AB, Alió JL (2014) Geometrical custom modeling of human cornea in vivo and its use for the diagnosis of corneal ectasia. PLoS ONE 9 (10). doi:10.1371/journal.pone.0110249
17. Wang L, Dai E, Koch DD, Nathoo A (2003) Optical aberrations of the human anterior cornea. Journal of Cataract and Refractive Surgery 29 (8):1514-1521. doi:10.1016/S0886-3350(03)00467-X
18. Hernández-Camarena JC, Chirinos-Saldaña P, Navas A, Ramirez-Miranda A, De La Mota A, Jimenez-Corona A, Graue-Hernández EO (2014) Repeatability, reproducibility, and agreement between three different scheimpflug systems in measuring corneal and anterior segment biometry. Journal of Refractive Surgery 30 (9):616-621. doi:10.3928/1081597X-20140815-02
19. Montalbán R, Piñero DP, Javaloy J, Alió JL (2012) Intrasubject repeatability of corneal morphology measurements obtained with a new Scheimpflug photography-based system. Journal of Cataract and Refractive Surgery 38 (6):971-977. doi:10.1016/j.jcrs.2011.12.029
20. Piñero DP, Alió JL, Alesón A, Vergara ME, Miranda M (2010) Corneal volume, pachymetry, and correlation of anterior and posterior corneal shape in subclinical and different stages of clinical keratoconus. Journal of Cataract and Refractive Surgery 36 (5):814-825. doi:10.1016/j.jcrs.2009.11.012
21. Ishii R, Kamiya K, Igarashi A, Shimizu K, Utsumi Y, Kumanomido T (2012) Correlation of corneal elevation with severity of keratoconus by means of anterior and posterior topographic analysis. Cornea 31 (3):253-258. doi:10.1097/ico.0b013e31823d1ee0